

## Development of Potent Carbonic Anhydrase Inhibitors Incorporating Both Sulfonamide and Sulfamide Groups

Katia D'Ambrosio,<sup>†</sup> Fatma-Zhora Smaine,<sup>‡</sup> Fabrizio Carta,<sup>§</sup> Giuseppina De Simone,<sup>†</sup> Jean-Yves Winum,<sup>\*,‡</sup> and Claudiu T. Supuran<sup>\*,§</sup>

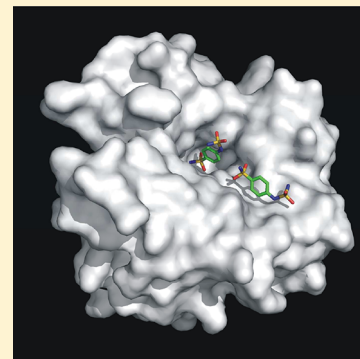
<sup>†</sup>Istituto di Biostrutture e Bioimmagini-CNR, via Mezzocannone 16, 80134 Napoli, Italy

<sup>‡</sup>Institut des Biomolécules Max Mousseron (IBMM), UMR 5247, CNRS-UM1-UM2 Bâtiment de Recherche Max Mousseron, Ecole Nationale Supérieure de Chimie de Montpellier, 8 rue de l'École Normale, 34296 Montpellier Cedex, France

<sup>§</sup>Università degli Studi di Firenze, Laboratorio di Chimica Bioinorganica, Rm. 188, Via della Lastruccia 3, I-50019 Sesto Fiorentino (Firenze), Italy

### S Supporting Information

**ABSTRACT:** A series of compounds incorporating both sulfonamide and sulfamide as zinc-binding groups (ZBGs) are reported as inhibitors of the metalloenzyme carbonic anhydrase (CA, EC 4.2.1.1). Crystallographic studies on the complex of hCA II with the lead compound of this series, namely, 4-sulfamido-benzenesulfonamide, revealed the binding of two molecules in the enzyme active site cavity, the first one canonically coordinated to the zinc ion by means of the sulfonamide group and the second one located at the entrance of the cavity. This observation led to the design of elongated molecules incorporating these two ZBGs, separated by a linker of proper length, to allow the simultaneous binding to these different sites. The “long” inhibitors indeed showed around 10 times better enzyme inhibitory properties as compared to the shorter molecules against four physiologically relevant human (h) isoforms, hCA I, II, IX, and XII.



### ■ INTRODUCTION

Carbonic anhydrases (CAs) are ubiquitous metallo-enzymes present in most living organisms and encoded by five evolutionarily unrelated gene families: the  $\alpha$ -,  $\beta$ -,  $\gamma$ -,  $\delta$ - and  $\zeta$ -CAs. Human CAs (hCAs) all belong to the  $\alpha$ -family and are present in 15 isoforms, which differ for tissue distribution, cellular localization, and kinetic properties. All of these enzymes catalyze the reversible hydration of carbon dioxide to bicarbonate and proton, a very simple reaction that is, however, of fundamental importance to many physiological processes based on gas exchange, ion transport, and pH balance. Consequently, hCAs are involved in a variety of physiological processes, and their abnormal levels and/or activities often have been associated with different human diseases.<sup>1–3</sup>

In the last years, CA isozymes have become an interesting target for the design of inhibitors or activators with biomedical applications.<sup>4–7</sup> Indeed, originally, CA inhibitors (CAIs) were clinically used as diuretic,<sup>8</sup> antiglaucoma,<sup>9</sup> anticonvulsant,<sup>10</sup> and antiobesity drugs,<sup>11</sup> whereas their employment in the management of hypoxic tumors was only recently validated,<sup>12–14</sup> with several monoclonal antibodies (Mabs)<sup>15</sup> and small molecule inhibitors in various stages of clinical development.<sup>15,16</sup> However, because of the large number of hCA isoforms,<sup>1–3</sup> there is a constant need to improve the inhibition and selectivity profile of the so far developed CAIs, to avoid side effects due to inhibition of isoforms not involved in a certain pathology.<sup>2</sup> In the last period, by using extensive drug design

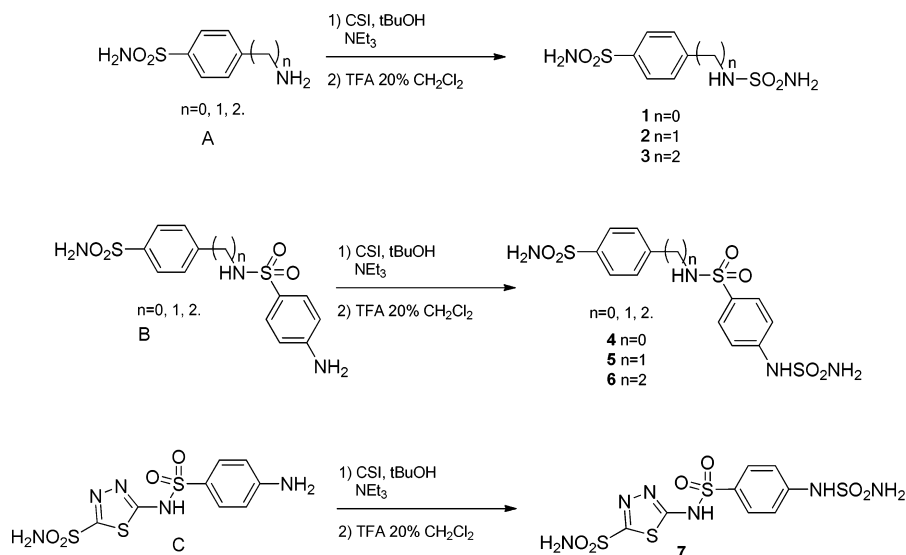
programs and with the help of X-ray crystallography,<sup>17</sup> much progress has been achieved.<sup>1–3</sup> Indeed, by considering the three main structural elements present in the molecule of a classical potent CAI, that is, a zinc-binding group (ZBG), an organic scaffold, and one or more side chains substituting the scaffold, important advances have been made in the understanding of the factors that govern both potency and selectivity against various hCA isozymes.

The ZBGs leading to potent CAIs may belong to various functionalities with the classical sulfonamide one still constituting the main player. The most obvious bioisosteres of this group are the sulfamate and sulfamide, in which an additional electron-withdrawing atom/group (O or NH, respectively) is directly attached to the sulfamoyl function, generating compounds with general formula R–O–SO<sub>2</sub>NH<sub>2</sub> or R–NH–SO<sub>2</sub>NH<sub>2</sub>. Such compounds were shown to lead equipotent, and in some cases even stronger, inhibitors than the corresponding sulfonamides. The X-ray structures of the two simplest compounds of such family, namely, sulfamide and sulfamic acid, in adduct with hCA II have been reported, showing that such molecules were able to participate to a more complicated hydrogen bond network with respect to that formed by the classical sulfonamide inhibitors, due to the presence of the additional oxygen/nitrogen atom.<sup>18</sup> At the

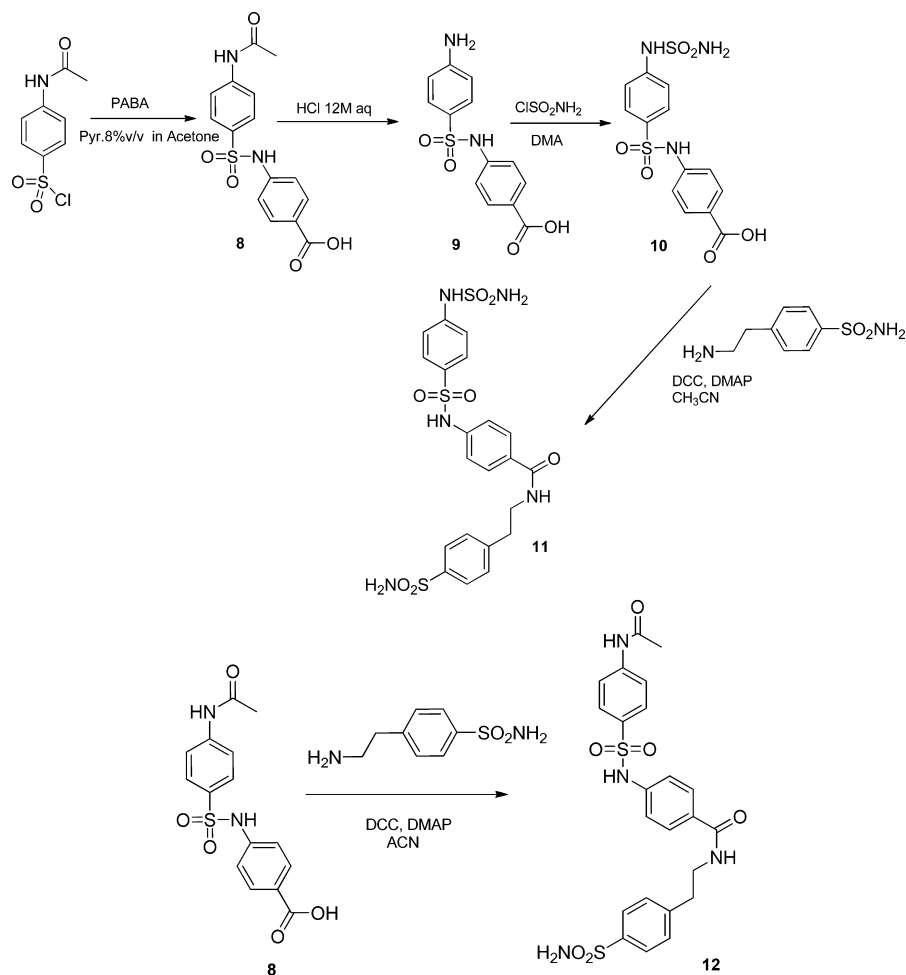
Received: February 13, 2012

Published: July 9, 2012

Scheme 1. Preparation of Compounds 1–7



Scheme 2. Synthesis of the “Long” CAIs 11 and 12



present time, there are a large number of aromatic, heterocyclic, aliphatic, and sugar-based sulfamates and sulfamides, which were shown to possess highly effective inhibitory properties against all known human isoforms.<sup>2</sup> Thus, also, the sulfamates and the sulfamides constitute a very important class of CAIs,

with some derivatives clinically used for the treatment of epilepsy and obesity.<sup>10,11,19–21</sup>

In this paper, we report a new series of CAIs incorporating in the same molecule two ZBGs, that is, the sulfonamide and sulfamide ones. The rationale behind our choice was to understand on one hand which of the two ZBGs could bind the

metal ion within the enzyme active site and, on the other hand, how the presence of two ZBGs in the same scaffold may influence the selectivity profile of the inhibitor against four of the major isoforms, the cytosolic CA I and II and the transmembrane, tumor-associated CA IX and XII.<sup>1–3,16</sup>

## RESULTS AND DISCUSSION

A straightforward chemistry has been used to prepare sulfonamides also incorporating sulfamide moieties of types 1–7 (Scheme 1). Simple aromatic sulfonamides possessing amino- or aminoalkyl moieties of type A, or their sulfonylated derivatives of types B and C,<sup>22,23</sup> were converted to the corresponding sulfamides by reaction with *N*-*tert*-butoxycarbonyl sulfamoylchloride [prepared *ab initio* by reaction of chlorosulfonyl isocyanate (CSI) with *tert*-butanol], followed by deprotection with trifluoroacetic acid (TFA), as reported earlier for simple amines.<sup>24</sup> Two other compounds, **11** and **12** (which will be called “long” CAIs), have been obtained as depicted in Scheme 2. *N*-Acetyl-sulfanyl chloride was treated with *p*-amino-benzoic acid (PABA), leading to **8**, which was deprotected in the presence of concentrated HCl to the amino derivative **9**.<sup>25,26</sup> This latter was then sulfamoylated using sulfamoylchloride as a reagent to give the sulfamide **10**. This compound, possessing a free COOH moiety, was reacted with 4-aminoethylbenzenesulfonamide and led to the first long CAI, compound **11** (the condensation was achieved by the classical dicyclohexyl carbodiimide chemistry). The key intermediate **8** was also condensed with 4-aminoethylbenzenesulfonamide in the same conditions and led to **12**, which differs from **11** by the presence of an acetamido moiety instead of the sulfamide one.

Before discussing the CA inhibitory data of compounds 1–12, we shall present a serendipitous crystallographic finding, which has triggered the preparation of the elongated compounds described here. We obtained crystals of the complex of hCA II with the simple sulfonamide-sulfamide derivative **1** ( $K_i$  of 74 nM, see later in the text). These crystals were isomorphous with those of the native protein,<sup>27</sup> which was then used as a starting model for crystallographic refinement after deletion of nonprotein atoms. Statistics for data collection and refinement are shown in Table 1. Inspection of the electron density maps, at various stages of crystallographic refinement, clearly showed the binding to the enzyme of three inhibitor molecules: one positioned on the protein surface far away from the active site, which will not be discussed in the following, and the other two located in the active site channel (Figure 1). The first one, entirely defined in the electron density maps (Figure 2), was located at the bottom of the active site and coordinated to Zn<sup>2+</sup> ion through its sulfonamide group. In particular, the ionized sulfonamide NH<sup>−</sup> group coordinated to the catalytic Zn<sup>2+</sup> ion with a tetrahedral geometry and donated a hydrogen bond to the Thr199OG1 atom (2.84 Å). One sulfonamide oxygen accepted a hydrogen bond from the backbone NH group of Thr199 (2.92 Å), while the other one was at a distance of 2.97 Å from the Zn<sup>2+</sup> ion. The binding through the sulfonamide moiety instead of the sulfamide one was probably due to the lower pK<sub>a</sub> value of the first one, allowing a much higher population of the anionic form, which is required for binding to Zn<sup>2+</sup>. The benzene ring of the inhibitor made a large number of strong (<4.5 Å) hydrophobic contacts with residues Gln92, His94, Val121, Phe131, Leu198, and Thr200. Finally, the sulfamide group in *para*-position to the coordinated sulfamoyl moiety did not interact with the protein but made

**Table 1. Crystal Parameters, Data Collection, and Refinement Statistics for the hCA II–1 Complex<sup>a</sup>**

| crystal parameters                        |  |
|---|--|
| space group                               | <i>P</i> 2 <sub>1</sub>  |
| unit cell parameters (Å, °)               | <i>a</i> = 42.25<br><i>b</i> = 41.35<br><i>c</i> = 71.96<br>$\beta$ = 104.36 |
| data collection statistics (20.00–1.50 Å) |  |
| temperature (K)                           | 100  |
| wavelength (Å)                            | 1.0000   |
| total reflections                         | 123249   |
| unique reflections                        | 38111  |
| completeness (%)                          | 98.2 (84.0)  |
| $R_{\text{merge}}^b$ (%)                  | 5.7 (20.6)   |
| mean $I/\sigma(I)$                        | 15.6 (4.9)   |
| refinement statistics (20.00–1.50 Å)      |  |
| $R_{\text{factor}}^c$ (%)                 | 18.6   |
| $R_{\text{free}}^c$ (%)                   | 21.2   |
| rmsd from ideal geometry:                 |  |
| bond lengths (Å)                          | 0.006  |
| bond angles (°)                           | 1.4  |
| no. of protein atoms                      | 2121   |
| no. of water molecules                    | 445  |
| no. of inhibitor atoms                    | 45   |
| average B factor                          | 11.75  |

<sup>a</sup>Values in parentheses refer to the highest resolution shell, 1.55–1.50 Å. <sup>b</sup> $R_{\text{merge}} = \sum_{hkl} \sum_i |I_i(hkl) - \langle I(hkl) \rangle| / \sum_{hkl} \sum_i I_i(hkl)$ , where  $I_i(hkl)$  is the intensity of an observation and  $\langle I(hkl) \rangle$  is the mean value for its unique reflection; summations are over all reflections. <sup>c</sup> $R_{\text{factor}} = \sum_h ||F_o(h) - |F_c(h)|| / \sum_h |F_o(h)|$ , where  $F_o$  and  $F_c$  are the observed and calculated structure-factor amplitudes, respectively.  $R_{\text{free}}$  was calculated with 5% of the data excluded from the refinement.

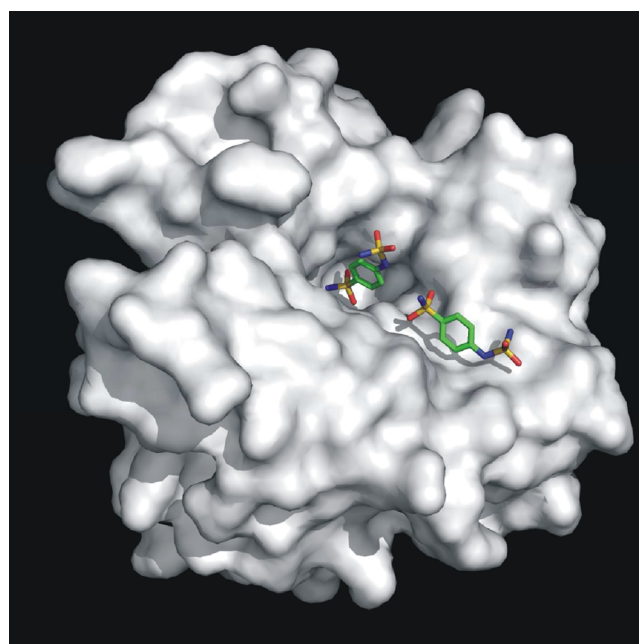


**Figure 1.** Solvent accessible surface of hCA II in its complex with **1**. The two molecules of **1** bound within the active site cavity are shown in stick representation.

a large number of hydrogen bond with several water molecules (Figure 3).

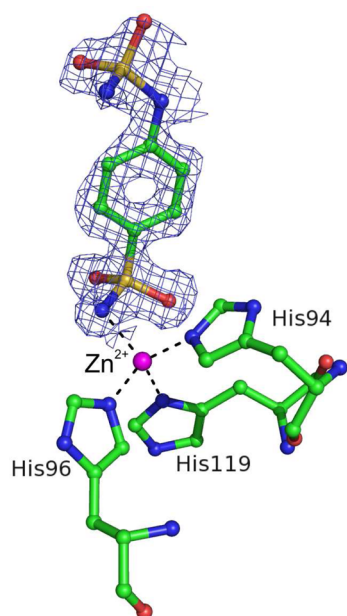


**Figure 2.** Simulated annealing omit  $2F_o - F_c$  electron density map, relative to the inhibitor molecule **1** coordinated to the catalytic zinc ion, which is also shown together with its coordinating residues.

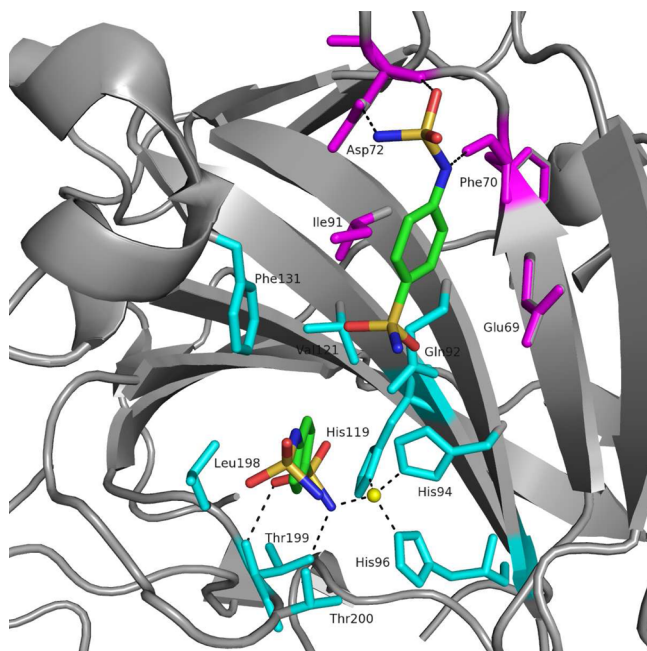


**Figure 3.** Ribbon diagram of the hCA II-1 complex. The two inhibitor molecules (green scaffold) bound within the active site are represented in stick representation. Residues participating in recognition of the inhibitor molecule bound to the catalytic zinc ion are reported in cyan, while those interacting with the external inhibitor molecule are shown in magenta. The active site  $Zn^{2+}$  coordination is also reported.

The second inhibitor molecule, which had lower interaction affinity with the enzyme (occupation factor = 0.7) (Figure 4), was located close to the protein surface, with the sulfonamide moiety pointing toward the interior of the active site and the sulfamide one oriented toward the external part of the cavity. The last group was the main player in stabilizing the binding of this inhibitor, forming three hydrogen bonds with the enzyme,

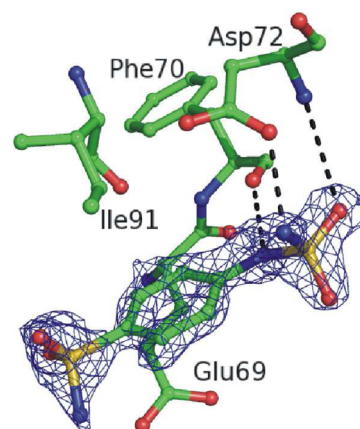


**Figure 4.** Simulated annealing omit  $2F_o - F_c$  electron density map, relative to the inhibitor molecule **1** located on the rim of the active site cavity. Residues involved in inhibitor recognition are also shown.

two of which with two main chain atoms (Figures 3 and 4). Additional hydrophobic interactions of the phenyl ring contributed to the stabilization of the binding, while the sulfonamide group did not interact directly with the enzyme. Altogether, these findings suggested that molecules containing a sulfonamide as ZBG, a linker of proper length, and a sulfamide able to interact with the border of the active site could show high affinity for the CA active site. To explore this hypothesis, we designed compound **11**, an elongated CAI, and compound **12**, which has the same length as **11** but possesses an acetamide instead of the sulfamide moiety present in **11**.

The inhibition data of all designed compounds against four human isoforms, namely, hCA I, II, IX, and XII, are reported in Tables 2 and 3.<sup>28</sup> Both the  $CO_2$  hydrase and the esterase assays (with 4-nitrophenylacetate as substrate) have been used,<sup>28</sup> as one of the reviewers suggested a different binding assay than monitoring only the inhibition of the physiologic reaction. Analysis of these inhibition data shows a very interesting inhibition profile for this newly designed series of compounds. For the  $CO_2$  hydrase assay, starting from the short inhibitors

**Table 2.** hCA I, II, IX, and XII Inhibition Data with Sulfonamides **1–12** and Standard Inhibitors AZA, EZA, and DCP by a Stopped-Flow,  $CO_2$  Hydration Assay Method<sup>28a</sup>

|           | $K_i$ (nM) <sup>a</sup> |                     |                     |                      |
|-----------|-------------------------|---------------------|---------------------|----------------------|
|           | hCA I <sup>b</sup>      | hCA II <sup>b</sup> | hCA IX <sup>c</sup> | hCA XII <sup>c</sup> |
| <b>1</b>  | 1130                    | 74                  | 64                  | 57                   |
| <b>2</b>  | 1425                    | 1170                | 65                  | 54                   |
| <b>3</b>  | 72                      | 59                  | 611                 | 580                  |
| <b>4</b>  | 633                     | 9.1                 | 27                  | 62                   |
| <b>5</b>  | 148                     | 178                 | 35                  | 53                   |
| <b>6</b>  | 43                      | 63                  | 65                  | 48                   |
| <b>7</b>  | 473                     | 62                  | 52                  | 79                   |
| <b>10</b> | 241                     | 49                  | 57                  | 43                   |
| <b>11</b> | 237                     | 0.6                 | 0.4                 | 0.5                  |
| <b>12</b> | 379                     | 5.2                 | 4.5                 | 3.9                  |
| AZA       | 250                     | 12                  | 25                  | 5.7                  |
| EZA       | 25                      | 8                   | 43                  | 56                   |
| DCP       | 1200                    | 38                  | 50                  | 50                   |

<sup>a</sup>Errors in the range of  $\pm 5$ –10% of the reported value from three different determinations. <sup>b</sup>Full length, cytosolic isoform. <sup>c</sup>Catalytic domain, recombinant enzyme.

**Table 3. hCA I and II Inhibition Data with Sulfonamides 1–12 and the Standard Inhibitors AZA by a Spectrophotometric Esterase Assay Method with 4-Nitrophenylacetate as the Substrate<sup>28b</sup>**

| compd | $K_i$ (nM) <sup>a</sup> |        |
|-------|-------------------------|--------|
|       | hCA I                   | hCA II |
| 1     | 1650                    | 123    |
| 2     | 1745                    | 1239   |
| 3     | 87                      | 68     |
| 4     | 950                     | 35     |
| 5     | 203                     | 182    |
| 6     | 75                      | 81     |
| 7     | 638                     | 80     |
| 10    | 327                     | 62     |
| 11    | 320                     | 5.3    |
| 12    | 384                     | 12.9   |
| AZA   | 342                     | 159    |

<sup>a</sup>Means from three different measurements.

1–3, it can be observed that compounds 1 and 2 were weak hCA I inhibitors ( $K_i$  values of 1.13–1.42  $\mu\text{M}$ ), while the longest molecule 3 was a medium potency inhibitor ( $K_i$  of 72 nM). Against hCA II, the profile was more complicated, with compounds 1 and 3 being medium potency inhibitors ( $K_i$  values of 59–74 nM), whereas the homosulfanilamide derivative 2 was a weak inhibitor ( $K_i$  of 1.17  $\mu\text{M}$ ). On the contrary, the tumor-associated isoforms hCA IX and XII were inhibited moderately by 1 and 2 ( $K_i$  values of 64–65 nM against CA IX and of 54–57 nM against CA XII, respectively), whereas the longer compound 3 was a weak inhibitor of both isoforms (Table 2).

The medium length compounds 4–7 generally showed an increase of their inhibitory capability against all isoforms as compared to the corresponding short inhibitors 1–3 with which they were structurally related. Indeed, against hCA I and II, an increase of the length of these molecules was generally reflected in a decrease of the  $K_i$  values. For example, by comparing the inhibition of hCA I with the pair 2 and 5, the last compound is 9.6 times a better inhibitor as compared to the short derivative 2. Against hCA II, the same compounds differ by a factor of 6.6 in inhibiting this isoform. Less differences were observed for the inhibition of hCA IX and especially hCA XII, for which some of the short molecules inhibitors (e.g., 1 and 2) showed comparable activity with the longer ones (4–6). Interestingly, for derivatives 4–7, compound 4, incorporating the sulfanilamide scaffold, is the best hCA II and IX inhibitor, even if it has a slightly shorter molecule as compared to its congeners 5 and 6. Thus, the structure–activity relationship (SAR) is rather complicated for derivatives 1–7, with the length of the molecule being an important factor but not the only one influencing enzyme inhibition. Furthermore, the four isoforms showed a rather different inhibition profile with these derivatives. All of these observations also can be applied to derivative 10, which incorporates PABA instead of the sulfanilamide moiety. This derivative has only the sulfamide as ZBG and shows medium potency inhibitory activity against all isoforms, with hCA IX, XII, and II being better inhibited than hCA I. The most interesting inhibition profile was observed with the long CAIs 11 and 12, designed on the basis of the observation that two molecules of 1 were bound within the hCA II active site. Indeed, as compared to 1, compound 11 was 123.3 times a better hCA II inhibitor, with an efficacy in the

subnanomolar range ( $K_i$  of 0.6 nM). This compound was also a subnanomolar inhibitor of hCA IX and XII, whereas its affinity for hCA I was 237 nM, not being much different from that of the medium length derivative 5. We thus consider that the hypothesis that led us to synthesize such a long molecule CAI has been verified, since we observe a huge inhibitory power increase (114–160 times) against the three CA isoforms of interest as drug targets, that is, hCA II, IX, and XII. It is interesting to note that compound 12, which has the same length as 11 but incorporates an acetamido instead of the sulfamide moiety, is still a potent hCA II, IX, and XII inhibitor ( $K_i$  values of 3.9–5.2 nM), even if slightly less efficient as compared to 11. It is thus probable that the sulfamide moiety present in 11, as the one from the second molecule of 1 bound to hCA II, participates in interactions with active site residues, to which the acetamido moiety cannot participate. It also may be observed that the long compounds 11 and 12 reported here are much better CAIs against all isoforms as compared to the clinically used derivatives acetazolamide (AZA), ethoxzolamide (EZA), and dichlorophenamide (DCP) (Table 2 and Figure 5).

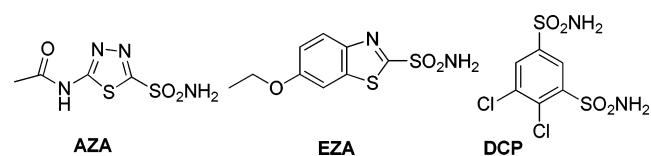


**Figure 5.** Chemical structures of classical CAIs AZA, EZA, and DCP.

The esterase inhibition data of Table 3 (against hCA I and II, as the transmembrane isoforms hCA IX and XII have much weaker esterase activity with 4-nitrophenyl acetate as substrate)<sup>28c</sup> very much parallel the  $\text{CO}_2$  hydrase inhibition data of Table 2, only that generally the  $K_i$  values are higher for the esterase method, a fact already reported by Pocker and Stone in 1967.<sup>28b</sup> Indeed, the short inhibitors were weaker than the long-tailed ones, confirming thus (by a distinct method) the data presented in Table 2 and discussed above.

## CONCLUSIONS

Here, we reported an interesting case of drug design of CAIs based on a serendipitous observation of two molecules of 4-sulfamido-benzenesulfonamide bound within the active site of hCA II. Although SAR for this family of inhibitors is not at all simple, an elongation of the molecules gradually led to increased inhibitory power, with the longest molecules being subnanomolar or low nanomolar inhibitors of hCA II, IX, and XII, whereas the inhibition of the off-target isoform hCA I remained in the micromolar range.

## EXPERIMENTAL SECTION

**Chemistry.** All reagents and solvents were of commercial quality and used without further purification, unless otherwise specified. All reactions were carried out under an inert atmosphere of nitrogen. TLC analyses were performed on silica gel 60 F<sub>254</sub> plates (Merck Art.1.05554). Spots were visualized under 254 nm UV illumination or by ninhydrin solution spraying. <sup>1</sup>H and <sup>13</sup>C NMR spectra were recorded on Bruker DRX-400 spectrometer using DMSO-*d*<sub>6</sub> as solvent and tetramethylsilane as internal standard. For <sup>1</sup>H NMR spectra, chemical shifts are expressed in  $\delta$  (ppm) downfield from tetramethylsilane, and coupling constants (*J*) are expressed in Hertz. Electron ionization mass spectra were recorded in positive or negative mode on a Water MicroMass ZQ. The purity of the obtained compounds was checked by HPLC and was >98%.

Compounds 1–7 were prepared according to the procedure described in ref 24 (see the Supporting Information). Starting material was commercially available or synthesized following procedures reported in refs 22 and 23.

**N-Sulfamoyl-4-aminobenzene Sulfonamide (1).** Yield: 80%. <sup>1</sup>H NMR (400 MHz, DMSO):  $\delta$  10.1 (s, 1H), 7.75 (d, 2H,  $J$  = 7.27 Hz), 7.35 (s, 2H), 7.25 (d, 2H,  $J$  = 7.27 Hz), 7.2 (s, 2H). MS ESI<sup>+</sup>/ESI<sup>-</sup>:  $m/z$  252.3 (M + H)<sup>+</sup>, 275.28 (M + Na)<sup>+</sup>, 250.3 (M - H)<sup>-</sup>. Anal. calcd for C<sub>6</sub>H<sub>9</sub>N<sub>3</sub>O<sub>4</sub>S<sub>2</sub>: C, 28.68; H, 3.61; N, 16.72. Found: C, 28.72; H, 3.64; N, 16.73. Detailed characterization of compounds 2–7 is provided in the Supporting Information.

**Synthesis of 4-(4-Acetamidophenylsulfonamido)benzoic Acid (8).**<sup>29</sup> N-Acetylsulfanylylchloride (10.48 g, 1.0 equiv) and 4-aminobenzoic acid (1.0 equiv) were suspended in dry acetone (42.0 mL) containing dry pyridine (8% v/v). The white mixture was stirred vigorously at r.t. until the starting material was consumed (TLC monitoring). Then, the reaction was quenched with H<sub>2</sub>O (60 mL) and triturated with 1.0 M aqueous hydrochloric acid to afford the titled product as a white solid that did not require further purification. Yield: 67%. Silica gel TLC  $R_f$  0.35 (MeOH/methylene chloride 20% v/v). <sup>1</sup>H NMR (400 MHz, DMSO-*d*<sub>6</sub>):  $\delta$  10.73 (s, 1H, exchange with D<sub>2</sub>O), 10.37 (s, 1H, exchange with D<sub>2</sub>O), 10.00 (brs, 1H, exchange with D<sub>2</sub>O), 7.82 (d, 2H,  $J$  = 8.4 Hz, Ar-H), 7.78 (m, 4H, Ar-H), 7.21 (d, 2H,  $J$  = 8.4 Hz, Ar-H), 2.09 (s, 3H, CH<sub>3</sub>). <sup>13</sup>C NMR (100 MHz, DMSO-*d*<sub>6</sub>): 170.1, 169.3, 144.0, 142.1, 136.3, 132.0, 130.1, 128.5, 119.1, 117.0, 22.5. Data are in agreement with reported data.<sup>29</sup>

**Synthesis of 4-(4-Aminophenylsulfonamido)benzoic Acid (9).**<sup>29</sup> 4-(4-Acetamidophenylsulfonamido)benzoic acid 8 (1.2 g) was suspended in 12 M aqueous hydrochloric acid, and the mixture was heated at reflux for 9 h and cooled down to r.t., and the pH adjusted to 3 by the addition of aqueous concentrated NH<sub>4</sub>OH. The precipitate formed was collected by filtration, dried under vacuo, and used for the next step as it is. Yield: 32%. Silica gel TLC  $R_f$  0.10 (MeOH/methylene chloride 20% v/v). <sup>1</sup>H NMR (400 MHz, DMSO-*d*<sub>6</sub>):  $\delta$  10.37 (s, 1H, exchange with D<sub>2</sub>O), 7.83 (d, 2H,  $J$  = 8.4 Hz, Ar-H), 7.79 (d, 2H,  $J$  = 8.4 Hz, Ar-H), 7.22 (d, 2H,  $J$  = 8.4 Hz, Ar-H), 7.58 (d, 2H,  $J$  = 8.4 Hz, Ar-H), 6.06 (brs, 2H, NH<sub>2</sub>). <sup>13</sup>C NMR (100 MHz, DMSO-*d*<sub>6</sub>): 170.0, 149.6, 145.0, 132.1, 130.0, 129.2, 118.4, 117.2, 116.8. Data are in agreement with reported data.<sup>29</sup>

**Synthesis of 4-(4-(Sulfamoylamino)phenylsulfonamido)benzoic Acid (10).**<sup>30</sup> 4-(4-Aminophenylsulfonamido)benzoic acid 9 (0.1 g, 1.0 eq) was dissolved in dry *N,N*-dimethylacetamide (5.0 mL) and treated with freshly prepared sulfamoyl chloride until starting material was consumed (TLC monitoring). Then, the solution was quenched with slush and extracted with ethyl acetate (4 × 15 mL). The combined organic layers were washed with brine (3 × 15 mL) and several times with H<sub>2</sub>O, dried over Na<sub>2</sub>SO<sub>4</sub>, filtered-off, and concentrated in vacuo to give a white residue that was triturated from methylene chloride to afford the titled compound as a white solid. Sulfamoyl chloride was prepared by modification of the method reported in literature.<sup>31</sup> Chlorosulfonylisocyanate (1.0 equiv) was dissolved into a minimal amount of dry methylene chloride at -10 °C, and then, formic acid was added dropwise. The white precipitate formed was treated under vacuo to eliminate all of the solvents and used as it is. Yield: 56%. <sup>1</sup>H NMR (400 MHz, DMSO-*d*<sub>6</sub>):  $\delta$  10.67 (s, 1H, exchange with D<sub>2</sub>O), 10.22 (s, 1H, exchange with D<sub>2</sub>O), 7.79 (d, 2H,  $J$  = 8.8 Hz, Ar-H), 7.72 (d, 2H,  $J$  = 8.8 Hz, Ar-H), 7.36 (s, 2H, exchange with D<sub>2</sub>O, SO<sub>2</sub>NH<sub>2</sub>), 7.21 (d, 2H,  $J$  = 8.8 Hz, Ar-H), 7.18 (d, 2H,  $J$  = 8.8 Hz, Ar-H). <sup>13</sup>C NMR (100 MHz, DMSO-*d*<sub>6</sub>): 167.8, 144.8, 143.2, 132.3, 131.8, 129.2, 126.4, 119.0, 117.6.

**Synthesis of 4-(4-(Sulfamoylamino)phenylsulfonamido)-N-(4-sulfamoyl-phenethyl)benzamide (11).** 4-(4-(Sulfamoylamino)phenylsulfonamido)benzoic acid 10 (0.15 g, 1.0 equiv) and 4-(2-aminoethyl)benzenesulfonamide (0.078 g, 1.0 equiv) were dissolved in dry acetonitrile (3.0 mL), and the reaction was treated with dicyclohexylcarbodiimide (0.088 g, 1.1 equiv) and 4-dimethylamino-pyridine (0.005 g, 0.1 equiv) and was stirred at r.t. until starting materials were consumed (TLC monitoring). Then, the mixture was quenched with H<sub>2</sub>O (20 mL) and was extracted with ethyl acetate (4 × 15 mL). The combined organic layers were dried over Na<sub>2</sub>SO<sub>4</sub>,

filtered-off, and concentrated in vacuo to give a solid residue that was purified by silica gel column chromatography eluting with 20% MeOH/methylene chloride v/v to afford the title compound as a light-brown solid. Yield: 45%. Silica gel TLC  $R_f$  0.22 (MeOH/methylene chloride 20% v/v). <sup>1</sup>H NMR (400 MHz, DMSO-*d*<sub>6</sub>):  $\delta$  10.55 (brs, 1H, exchange with D<sub>2</sub>O), 10.22 (s, 1H, exchange with D<sub>2</sub>O), 8.46 (t, 1H,  $J$  = 6.0 Hz, exchange with D<sub>2</sub>O, CONH), 7.77 (d, 2H,  $J$  = 8.8 Hz, Ar-H), 7.74 (d, 2H,  $J$  = 8.8 Hz, Ar-H), 7.69 (d, 2H,  $J$  = 8.8 Hz, Ar-H), 7.44 (d, 2H,  $J$  = 8.8 Hz, Ar-H), 7.39 (s, 2H, exchange with D<sub>2</sub>O, SO<sub>2</sub>NH<sub>2</sub>), 7.31 (s, 2H, exchange with D<sub>2</sub>O, SO<sub>2</sub>NH<sub>2</sub>), 7.23 (d, 2H,  $J$  = 8.8 Hz, Ar-H), 7.17 (d, 2H,  $J$  = 8.8 Hz, Ar-H), 3.48 (q, 2H,  $J$  = 6.0 Hz, CH<sub>2</sub>CH<sub>2</sub>NH), 2.91 (t, 2H,  $J$  = 6.0 Hz, CH<sub>2</sub>CH<sub>2</sub>NH). <sup>13</sup>C NMR (100 MHz, DMSO-*d*<sub>6</sub>): 166.7, 144.8, 144.7, 143.1, 141.6, 132.4, 130.6, 130.2, 129.4, 129.2, 126.8, 119.2, 117.6, 35.9, 31.8. The synthesis and characterization of 12 is provided in the Supporting Information.

**CA Inhibition. CO<sub>2</sub> Hydrase Assay.** An Applied Photophysics stopped-flow instrument has been used for assaying the CA-catalyzed CO<sub>2</sub> hydration activity.<sup>28a</sup> Phenol red (at a concentration of 0.2 mM) has been used as an indicator, working at the absorbance maximum of 557 nm, with 20 mM Hepes (pH 7.5) as buffer, and 20 mM Na<sub>2</sub>SO<sub>4</sub> (for maintaining constant the ionic strength), following the initial rates of the CA-catalyzed CO<sub>2</sub> hydration reaction for a period of 10–100 s. The CO<sub>2</sub> concentrations ranged from 1.7 to 17 mM for the determination of the kinetic parameters and inhibition constants. For each inhibitor, at least six traces of the initial 5–10% of the reaction have been used for determining the initial velocity. The uncatalyzed rates were determined in the same manner and subtracted from the total observed rates. Stock solutions of inhibitor (0.1 mM) were prepared in distilled–deionized water, and dilutions up to 0.01 nM were done thereafter with distilled–deionized water. Inhibitor and enzyme solutions were preincubated together for 15 min at room temperature prior to assay, to allow for the formation of the E–I complex. The inhibition constants were obtained by nonlinear least-squares methods using PRISM 3 and represent the mean from at least three different determinations. CA isoforms were recombinant ones obtained in house as reported earlier.

**Esterase Assay.** Initial rates of 4-nitrophenyl acetate hydrolysis catalyzed by different CA isozymes were monitored spectrophotometrically, at the isosbestic point (347 nm), with a Cary 3 instrument interfaced with an IBM compatible PC.<sup>28b</sup> Solutions of substrate were prepared in anhydrous acetonitrile; the substrate concentrations varied between 2.10<sup>-2</sup> and 1.10<sup>-6</sup> M, working at 25 °C. A molar absorption coefficient  $\epsilon$  of 18400 M<sup>-1</sup> cm<sup>-1</sup> was used for the 4-nitrophenolate formed by hydrolysis, in the conditions of the experiments (pH 7.40), as reported by Pocker and Stone.<sup>28b</sup> Nonenzymatic hydrolysis rates were always subtracted from the observed rates. Duplicate experiments were done for each inhibitor concentration, and the values reported throughout the paper are the mean of such results. Stock solutions of inhibitor (1 mM) were prepared in distilled–deionized water with 10% (v/v) DMSO (which is not inhibitory at these concentrations), and dilutions up to 0.01 nM were done thereafter with distilled–deionized water. Inhibitor and enzyme solutions were preincubated together for 10 min at room temperature prior to assay, to allow for the formation of the E–I complex. The inhibition constant  $K_i$  was determined as described by Pocker and Stone.<sup>28b</sup> Enzyme concentrations were 3.2 nM for hCA II and 11 nM for hCA I (isoforms hCA IX and XII have a much lower esterase activity than hCA I and II and were not assayed by this method).

**Crystallization, X-ray Data Collection, and Structure Resolution.** The hCA II–I complex was obtained by adding a 5 M excess of inhibitor to a 10 mg/mL protein solution in 100 mM Tris-HCl buffer, pH 8.5. Crystals of the complex were grown at 20 °C by the vapor diffusion hanging drop method. Drops were prepared by mixing equal volumes of complex (10 mg/mL in 0.1 M TRIS-HCl pH 8.5) and precipitant solution, which contained 2.5 M (NH<sub>4</sub>)<sub>2</sub>SO<sub>4</sub>, 0.3 M NaCl, 100 mM Tris-HCl (pH 8.2), and 5 mM 4-(hydroxymercuribenzoic) acid. Crystals grew within a few days and were isomorphous to those of the native enzyme.<sup>27</sup> X-ray diffraction data were collected to 1.50 Å resolution at the Synchrotron source Elettra in Trieste, using a Mar CCD detector. Prior to cryogenic freezing, the crystals were

transferred to the precipitant solution with the addition of 15% (v/v) glycerol. Diffracted data were processed using the HKL crystallographic data reduction package.<sup>32</sup> Diffraction data were indexed in the  $P2_1$  space group with one molecule in the asymmetric unit. Unit cell parameters and data reduction statistics are summarized in Table 1. The enzyme–inhibitor complex structure was analyzed by difference Fourier techniques, using the atomic coordinates of the native hCA II (PDB entry 1CA2)<sup>27</sup> as a starting model. The refinement was carried out with the program CNS,<sup>33</sup> whereas the model building and map inspection were performed using the O program.<sup>34</sup> Inspection of the electron density maps, at various stages of crystallographic refinement, clearly showed the binding of three inhibitor molecules: one positioned on the protein surface far away from the active site and the other two located in the active site channel (Figures 1–4). After initial refinement limited to the enzyme, inhibitor molecules were gradually built into the model for further refinement. Restraints on inhibitor bond angles and distances were taken from similar structures in the Cambridge Structural Database, and standard restraints were used on protein bond angles and distances throughout refinement. The ordered water molecules were added automatically and checked individually. Each peak contoured at  $3\sigma$  in the  $|F_o| - |F_c|$  maps was identified as a water molecule, provided that hydrogen bonds would be allowed between this site and the model. The correctness of stereochemistry was finally checked using PROCHECK.<sup>35</sup> Final refinement statistics are reported in Table 1. Coordinates and structure factors have been deposited with the Protein Data Bank (accession code 3V5G). All figures were drawn using Pymol.<sup>36</sup>

## ■ ASSOCIATED CONTENT

### 📄 Supporting Information

Detailed characterization of compounds 2–7 and 12. This material is available free of charge via the Internet at <http://pubs.acs.org>.

## ■ AUTHOR INFORMATION

### Corresponding Author

\*Tel: +33 467-14-72-34. Fax: +33 467-14-43-44. E-mail: jeanyves.winum@univ-montp2.fr (J.-Y.W.). Tel: +39-055-4573005. Fax: +39-055-4573385. E-mail: claudiu.supuran@unifi.it (C.T.S.).

### Notes

The authors declare no competing financial interest.

## ■ ACKNOWLEDGMENTS

The financial support by the CNRS/CNR (CoopIntEER program, Grant No. 131999 to G.D.S. and J.-Y.W.) and from the EU FP7 project Metoxia (to C.T.S.) are gratefully acknowledged.

## ■ ABBREVIATIONS USED

CA, carbonic anhydrase; CAI, CA inhibitor; CSI, chlorosulfonyl isocyanate; hCA, human CA; PABA, *p*-amino-benzoic acid; ZBG, zinc-binding group

## ■ REFERENCES

- (1) Alterio, V.; Di Fiore, A.; D'Ambrosio, K.; Supuran, C. T.; De Simone, G. Multiple Binding Modes of Inhibitors to Carbonic Anhydrases: How to Design Specific Drugs Targeting 15 Different Isoforms? *Chem. Rev.* **2012**, *112*, DOI: 10.1021/cr200176r.
- (2) (a) Supuran, C. T. Carbonic anhydrases: Novel therapeutic applications for inhibitors and activators. *Nat. Rev. Drug Discovery* **2008**, *7*, 168–181. (b) Supuran, C. T. Carbonic anhydrase inhibitors and activators for novel therapeutic applications. *Future Med. Chem.* **2011**, *3*, 1165–1180.
- (3) Mack, E. T.; Snyder, P. W.; Perez-Castillejos, R.; Bilgicer, B.; Moustakas, D. T.; Butte, M. J.; Whitesides, G. M. Dependence of

Avidity on Linker Length for a Bivalent Ligand-Bivalent Receptor Model System. *J. Am. Chem. Soc.* **2012**, *134*, 333–345.

(4) Winum, J. Y.; Vullo, D.; Casini, A.; Montero, J. L.; Scozzafava, A.; Supuran, C. T. Carbonic anhydrase inhibitors. Inhibition of cytosolic isozymes I and II and transmembrane, tumor-associated isozyme IX with sulfamates including EMATE also acting as steroid sulfatase inhibitors. *J. Med. Chem.* **2003**, *46*, 2197–2204.

(5) Abbate, F.; Winum, J. Y.; Potter, B. V.; Casini, A.; Montero, J. L.; Scozzafava, A.; Supuran, C. T. Carbonic anhydrase inhibitors: X-ray crystallographic structure of the adduct of human isozyme II with EMATE, a dual inhibitor of carbonic anhydrases and steroid sulfatase. *Bioorg. Med. Chem. Lett.* **2004**, *14*, 231–234.

(6) Winum, J. Y.; Scozzafava, A.; Montero, J. L.; Supuran, C. T. Design of zinc binding functions for carbonic anhydrase inhibitors. *Curr. Pharm. Des.* **2008**, *14*, 615–621.

(7) Winum, J. Y.; Scozzafava, A.; Montero, J. L.; Supuran, C. T. Therapeutic potential of sulfamides as enzyme inhibitors. *Med. Res. Rev.* **2006**, *26*, 767–792.

(8) Supuran, C. T. Diuretics: From classical carbonic anhydrase inhibitors to novel applications of the sulfonamides. *Curr. Pharm. Des.* **2008**, *14*, 641–648.

(9) Mincione, F.; Scozzafava, A.; Supuran, C. T. In *Drug Design of Zinc-Enzyme Inhibitors: Functional, Structural, and Disease Applications*; Supuran, C. T., Winum, J. Y., Eds.; Wiley: Hoboken, 2009; pp 139–154.

(10) Thiry, A.; Dogné, J. M.; Masereel, B.; Supuran, C. T. Carbonic Anhydrase Inhibitors as Anticonvulsant Agents. *Curr. Top. Med. Chem.* **2007**, *7*, 855–864.

(11) De Simone, G.; Di Fiore, A.; Supuran, C. T. Are carbonic anhydrase inhibitors suitable for obtaining antiobesity drugs? *Curr. Pharm. Des.* **2008**, *14*, 655–660.

(12) Dubois, L.; Lieuwes, N. G.; Maresca, A.; Thiry, A.; Supuran, C. T.; Scozzafava, A.; Wouters, B. G.; Lambin, P. Imaging of CA IX with fluorescent labelled sulfonamides distinguishes hypoxic and (re)-oxygenated cells in a xenograft tumour model. *Radiother. Oncol.* **2009**, *92*, 423–428.

(13) Ahlskog, J. K.; Dumelin, C. E.; Trüssel, S.; Marling, J.; Neri, D. In vivo targeting of tumor-associated carbonic anhydrases using acetazolamide derivatives. *Bioorg. Med. Chem. Lett.* **2009**, *19*, 4851–4856.

(14) Buller, F.; Steiner, M.; Frey, K.; Mircsof, D.; Scheuermann, J.; Kalisch, M.; Bühlmann, P.; Supuran, C. T.; Neri, D. Selection of Carbonic Anhydrase IX Inhibitors from One Million DNA-Encoded Compounds. *ACS Chem. Biol.* **2011**, *6*, 336–344.

(15) Zatovicova, M.; Jelenska, L.; Hulikova, A.; Csaderova, L.; Ditte, Z.; Ditte, P.; Goliassova, T.; Pastorek, J.; Pastorekova, S. Carbonic anhydrase IX as an anticancer therapy target: Preclinical evaluation of internalizing monoclonal antibody directed to catalytic domain. *Curr. Pharm. Des.* **2010**, *16*, 3255–3263.

(16) Neri, D.; Supuran, C. T. Interfering with pH regulation in tumours as a therapeutic strategy. *Nat. Rev. Drug Discovery* **2011**, *10*, 767–777.

(17) Alterio, V.; Di Fiore, A.; D'Ambrosio, K.; Supuran, C. T.; De Simone, G. In *Drug Design of Zinc-Enzyme Inhibitors: Functional, Structural, and Disease Applications*; Supuran, C. T., Winum, J. Y., Eds.; Wiley: Hoboken, 2009; pp 73–138.

(18) Abbate, F.; Supuran, C. T.; Scozzafava, A.; Orioli, P.; Stubbs, M. T.; Klebe, G. Nonaromatic sulfonamide group as an ideal anchor for potent human carbonic anhydrase inhibitors: role of hydrogen-bonding networks in ligand binding and drug design. *J. Med. Chem.* **2002**, *45*, 3583–3587.

(19) De Simone, G.; Supuran, C. T. Antiobesity carbonic anhydrase inhibitors. *Curr. Top. Med. Chem.* **2007**, *7*, 879–884.

(20) Supuran, C. T.; Di Fiore, A.; De Simone, G. Carbonic anhydrase inhibitors as emerging drugs for the treatment of obesity. *Expert Opin. Emerging Drugs* **2008**, *13*, 383–392.

(21) Thiry, A.; Dogné, J. M.; Supuran, C. T.; Masereel, B. Anticonvulsant sulfonamides/sulfamates/sulfamides with carbonic

anhydrase inhibitory activity: Drug design and mechanism of action. *Curr. Pharm. Des.* **2008**, *14*, 661–671.

(22) Cecchi, A.; Winum, J. Y.; Innocenti, A.; Vullo, D.; Montero, J. L.; Scozzafava, A.; Supuran, C. T. Carbonic anhydrase inhibitors: Synthesis and inhibition of cytosolic/tumor-associated carbonic anhydrase isozymes I, II, and IX with sulfonamides derived from 4-isothiocyanato-benzolamide. *Bioorg. Med. Chem. Lett.* **2004**, *14*, 5775–5780.

(23) Puccetti, L.; Fasolis, G.; Cecchi, A.; Winum, J. Y.; Gamberi, A.; Montero, J. L.; Scozzafava, A.; Supuran, C. T. Carbonic anhydrase inhibitors: Synthesis and inhibition of cytosolic/tumor-associated carbonic anhydrase isozymes I, II, and IX with sulfonamides incorporating thioureido-sulfanyl scaffolds. *Bioorg. Med. Chem. Lett.* **2005**, *15*, 2359–2364.

(24) Casini, A.; Winum, J. Y.; Montero, J. L.; Scozzafava, A.; Supuran, C. T. Carbonic anhydrase inhibitors: Inhibition of cytosolic isozymes I and II with sulfamide derivatives. *Bioorg. Med. Chem. Lett.* **2003**, *13*, 837–840.

(25) Supuran, C. T.; Clare, B. W. Carbonic anhydrase inhibitors. Part 24. A quantitative structure–activity study of positively-charged sulfonamide inhibitors. *Eur. J. Med. Chem.* **1995**, *30*, 687–696.

(26) Supuran, C. T.; Clare, B. W. Carbonic anhydrase inhibitors. Part 57. Quantum chemical QSAR of a group of 1,3,4-thiadiazole and 1,3,4-thiadiazoline disulfonamides with carbonic anhydrase inhibitory properties. *Eur. J. Med. Chem.* **1999**, *34*, 41–50.

(27) Eriksson, A. E.; Jones, T. A.; Liljas, A. Refined structure of human carbonic anhydrase II at 2.0 Å resolution. *Proteins* **1988**, *4*, 274–282.

(28) (a) Khalifah, R. G. The carbon dioxide hydration activity of carbonic anhydrase. I. Stop-flow kinetic studies on the native human isoenzymes B and C. *J. Biol. Chem.* **1971**, *246*, 2561–2573. (b) Pocker, Y.; Stone, J. T. The catalytic versatility of erythrocyte carbonic anhydrase. III. Kinetic studies of the enzyme-catalyzed hydrolysis of p-nitrophenyl acetate. *Biochemistry* **1967**, *6*, 668–678. (c) Innocenti, A.; Supuran, C. T. Paraoxon, 4-nitrophenyl phosphate and acetate are substrates of  $\alpha$ - but not of  $\beta$ -,  $\gamma$ - and  $\zeta$ -carbonic anhydrases. *Bioorg. Med. Chem. Lett.* **2010**, *20*, 6208–6212.

(29) Pastor-Navarro, N.; García-Bover, C.; Maquieira, A.; Puchades, R. Specific polyclonal-based immunoassays for sulfathiazole. *Anal. Bioanal. Chem.* **2004**, *379*, 1088–1099.

(30) Okada, M.; Iwashita, S.; Koizumi, N. Efficient general method for sulfamoylation of a hydroxyl group. *Tetrahedron Lett.* **2000**, *41*, 7047–7051.

(31) Appel, R.; Berger, G. Hydrazodiazulfamides. *Chem. Ber.* **1958**, *91*, 1339–1341.

(32) Otwinowski, Z.; Minor, W. Processing of X-ray Diffraction Data Collected in Oscillation Mode. *Methods Enzymol.* **1997**, *276*, 307–326.

(33) Brunger, A. T.; Adams, P. D.; Clore, G. M.; De Lano, W. L.; Gros, P.; Grosse-Kunstleve, R. W.; Jiang, J. S.; Kuszewski, J.; Nilges, M.; Pannu, N. S.; Read, R. J.; Rice, L. M.; Simonson, T.; Warren, G. L. Crystallography & NMR system: A new software suite for macromolecular structure determination. *Acta Crystallogr., Sect. D* **1998**, *54*, 905–921.

(34) Jones, T. A.; Zou, J. Y.; Cowan, S. W.; Kjeldgaard, M. Improved methods for building protein models in electron density maps and the location of errors in these models. *Acta Crystallogr., Sect. A* **1991**, *47*, 110–119.

(35) Laskowski, R. A.; MacArthur, M. W.; Moss, D. S.; Thornton, J. M. PROCHECK: A program to check the stereochemical quality of protein structures. *J. Appl. Crystallogr.* **1993**, *26*, 283–291.

(36) The PyMOL Molecular Graphics System, Version 1.5.0.1, Schrödinger, LLC.